MOLECULAR ECOLOGY

Molecular Ecology (2016) doi: 10.1111/mec.13661

Transcriptomic plasticity in brown adipose tissue contributes to an enhanced capacity for nonshivering thermogenesis in deer mice

JONATHAN P. VELOTTA,[1] JENNIFER JONES,[2] COLE J. WOLF[1] and ZACHARY A. CHEVIRON[1]

Department of Animal Biology, University of Illinois at Urbana-Champaign, Urbana, IL 61081, USA

Abstract

For small mammals living at high altitude, aerobic heat generation (thermogenesis) is essential for survival during prolonged periods of cold, but is severely impaired under conditions of hypobaric hypoxia. Recent studies in deer mice (*Peromyscus maniculatus*) reveal adaptive enhancement of thermogenesis in high- compared to low-altitude populations under hypoxic cold stress, an enhancement that is attributable to modifications in the aerobic metabolism of muscles used in shivering. However, because small mammals rely heavily on nonshivering mechanisms for cold acclimatization, we tested for evidence of adaptive divergence in nonshivering thermogenesis (NST) under hypoxia. To do so, we measured NST and characterized transcriptional profiles of brown adipose tissue (BAT) in high- and low-altitude deer mice that were (i) wild-caught and acclimatized to their native altitude, and (ii) born and reared under common garden conditions at low elevation. We found that NST performance under hypoxia is enhanced in wild-caught, high-altitude deer mice, a difference that is associated with increased expression of coregulated genes that influence several physiological traits. These traits include vascularization and O_2 supply to BAT, brown adipocyte proliferation and the uncoupling of oxidative phosphorylation from ATP synthesis in the generation of heat. Our results suggest that acclimatization to hypoxic cold stress is facilitated by enhancement of nonshivering heat production, which is driven by regulatory plasticity in a suite of genes that influence intersecting physiological pathways.

Keywords: evolutionary genomics, high-altitude adaptation, regulatory networks, RNA-seq, thermogenic capacity, thermoregulation, WGCNA

Received 17 November 2015; revision received 4 March 2016; accepted 1 April 2016

Introduction

An understanding of the mechanisms by which organisms solve complex physiological problems allows for deep insight into the causes of adaptive evolution (Garland & Carter 1994; Dalziel *et al.* 2009; Storz & Wheat 2010). Many adaptive traits, especially those involved in energy metabolism, require continuous modifications of dynamic physiological processes, as well as the wholesale modification of energy usage and/or O_2 flux to tissues (e.g. Cheviron *et al.* 2012, 2013, 2014). One way to uncover the mechanistic basis of such adaptive traits is by linking variation in genomewide transcriptional regulation to physiology and fitness in a comparative framework (e.g. Whitehead *et al.* 2011; Cheviron *et al.* 2012, 2014; Whitehead 2012; Scott *et al.* 2015). Animals inhabiting high-altitude environments are particularly well suited for studies that integrate functional genomics, physiology and adaptive evolution in a mechanistic light because the unremitting hypoxia and extreme cold temperatures place intense selection pressures on

Correspondence: Jonathan P. Velotta, Fax: (406) 243 4184; E-mail: jonathan.velotta@gmail.com

[1]Present address: Division of Biological Sciences, University of Montana, Missoula, MT 59812, USA

[2]Present address: Department of Biochemistry, Midwestern University, Downers Grove, IL 60515, USA

the organisms that live under these conditions. Studies of the unique physiologies of high-altitude species provide clear examples of adaptive phenotypic evolution (Beall 2000, 2007; Storz 2007; Storz *et al.* 2010b; Cheviron & Brumfield 2012).

At high altitude, chronic O_2 deprivation places well-documented constraints on maximal aerobic metabolism of animals, thereby severely limiting their capacity for aerobic heat production (thermogenesis; Rosenmann & Morrison 1974; Hayes & Chappell 1986; Chappell *et al.* 1988, 2007; Ward *et al.* 1989; Hammond *et al.* 2002; Chappell & Hammond 2003). This is a particularly severe challenge for small, winter-active mammals that depend on aerobic thermogenesis for survival during periods of prolonged cold stress (Conley & Porter 1986). Indeed, estimates of field metabolic rates suggest that deer mice (*Peromyscus maniculatus*) living at high elevation operate very near the limits of their aerobic performance capabilities while active (Hayes 1989). Consistent with expected fitness effects, mark and recapture studies suggest strong directional selection on thermogenic capacity in high-altitude deer mice, as animals with higher capacities for aerobic thermogenesis were more likely to survive intense periods of cold (Hayes & O'Connor 1999). Correspondingly, a population of highland deer mice from the Colorado Rockies exhibits consistently higher thermogenic capacities under hypoxia compared to mice from a lowland Nebraskan prairie, a difference that seems to have a constitutive genetic basis (Cheviron *et al.* 2013).

In determining the mechanistic causes of this adaptive enhancement of thermogenic capacity under hypoxia, previous research has focused on the contribution of skeletal muscles used in shivering thermogenesis. In comparison with lowland deer mice, highland mice have evolved an increased capacity to oxidize lipids as a primary fuel source during aerobic thermogenesis under hypoxia, as well as an increase in skeletal muscle enzyme activity that is associated with concerted changes in gene expression across fatty acid oxidation and oxidative phosphorylation pathways (Cheviron *et al.* 2012). Greater thermogenic capacities in high-altitude mice are strongly correlated with upregulation of genes that contribute to O_2 diffusion and utilization by skeletal muscles, as well as constitutive increases in muscle oxidative capacity, capillarity and maximal oxidative enzyme activity (Cheviron *et al.* 2014; Lui *et al.* 2015; Scott *et al.* 2015).

Although a number of studies have identified skeletal muscle adaptations that likely enhance the capacity for shivering thermogenesis, little is known of the role of nonshivering thermogenesis (NST) in high-altitude adaptation, despite that fact that it is a critical component of cold acclimatization in small mammals (Janský 1973; Himms-Hagen 1985; Heldmaier *et al.* 1989; Cannon & Nedergaard 2004), and may account for more than 50% of overall thermogenic capacity in deer mice (Van Sant & Hammond 2008). The process of generating heat via NST involves the uncoupling of oxidative phosphorylation from ATP synthesis through the action of a highly specialized protein known as uncoupling protein 1 (UCP1), within brown adipose tissue (BAT; Nedergaard *et al.* 2001; Cannon & Nedergaard 2004, 2011). This process is mediated by a cascade of events beginning with the cold-induced stimulation of norepinephrine (reviewed in Cannon & Nedergaard 2004; Fig. 1). In short, norepinephrine (NE) stimulates a host of responses that facilitate NST, including vascular endothelial growth factor (VEGF) pathway expression (which promotes O_2 and fuel supply to BAT), and cellular differentiation of brown pre-adipocytes into mature brown adipocytes. NE stimulation of the β_3 adrenergic receptor initiates a signalling cascade leading to increased transcription of the *Ucp1* gene, and inhibition of apoptosis, which increases brown adipocyte proliferation. This cascade also triggers the release of fatty acids from triglycerides (lipolysis), which are used in β-oxidation and citric acid cycles. The distinct feature of cellular respiration in BAT is that the proton gradient generated from this reaction is not used to produce ATP, but is instead recycled through available UCP1. The combustion generated in this process produces heat (Fig. 1).

The extent to which functional modification of NST within BAT contributes to physiological acclimatization or genetic adaptation to hypoxic cold stress is not known, but may involve regulatory changes to pathways at several hierarchical levels, including BAT O_2 supply and utilization, proliferation and differentiation of brown adipocytes, and the cellular cascade that leads to uncoupling of oxidative phosphorylation. Because these pathways have been well characterized, an examination of their differential regulation in highland and lowland deer mice can be used to infer the mechanistic basis of adaptive enhancement of NST in response to hypoxic cold stress.

In this study, we aimed to determine whether high-altitude deer mice have evolved a greater capacity for NST under hypoxia compared to their lowland counterparts. Such an effect would complement evolved differences in muscle phenotype that putatively enhance the capacity for shivering thermogenesis. We then examined the regulatory changes within BAT that contribute to population-level variation in NST.

We measured NST performance of highland and lowland deer mice that were (i) wild-caught and acclimatized to their native habitat (in situ) and (ii) the F_1 progeny of wild-caught mice that were born and reared

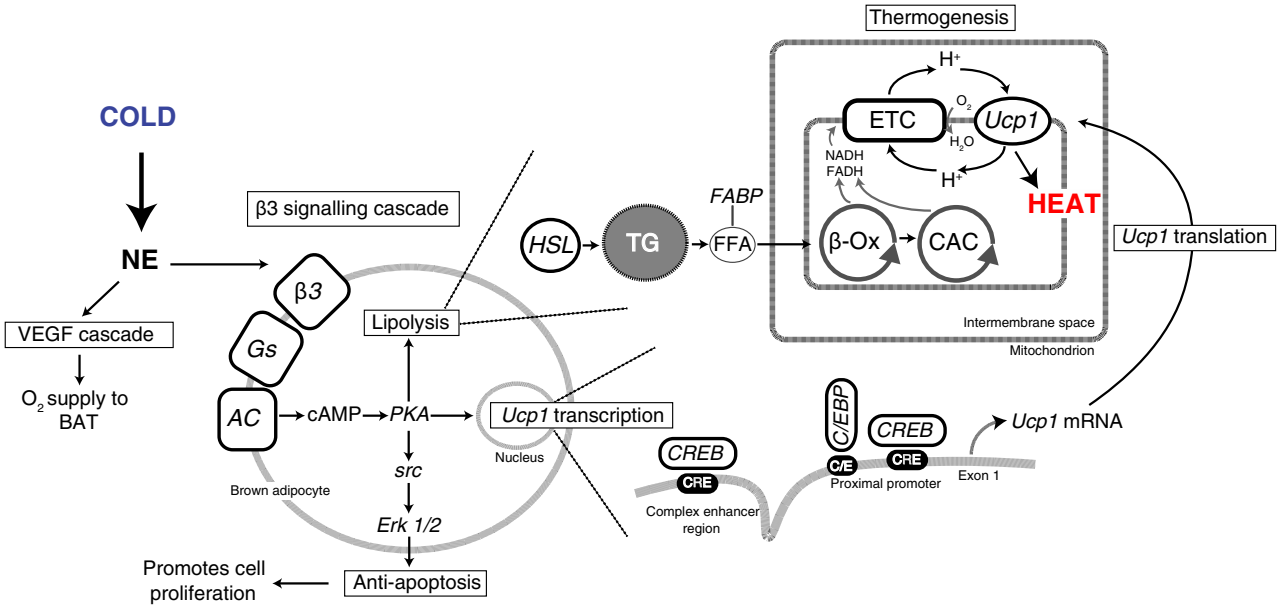

Fig. 1 Schematic representation of cold-induced norepinephrine (NE) signalling and key regulatory pathways leading to enhanced nonshivering thermogenesis within brown adipocytes. NE stimulates VEGF signalling, which promotes O_2 supply to BAT. NE further activates the β3 adrenergic receptor (β3) signalling cascade, which induces *Ucp1* transcription, lipolysis and apoptosis inhibition. The β3 signal is transduced via stimulatory G protein (G_s), adenylyl cyclase (AC), cAMP and protein kinase A (PKA). PKA phosphorylates cAMP response element binding protein (CREB), which binds to CRE sites in the promoter and enhancer region of the *Ucp1* gene, resulting in upregulation of its transcription. PKA also activates nuclear receptor co-activator (src), which then activates the Erk 1/2 pathway, leading to the inhibition of apoptosis and promotes cell proliferation. PKA activation leads to lipolysis, whereby phosphorylated hormone sensitive lipases (HSL) liberate free fatty acids (FFA) from triglycerides (TG). FFAs are transported by fatty acid binding proteins (FAPB) and used as fuel in the ensuing β-oxidation (β-ox), citric acid cycle (CAC) and electron transport chain (ETC.). Resulting H^+ is recycled through Ucp1 instead of ATP synthase, which generates heat as a by-product. Figure modified from Cannon & Nedergaard (2004).

under common garden, low-elevation conditions. This design allowed us to control for environmental influences on NST performance, including plasticity in BAT proliferation and oxidative capacity. We then sequenced the BAT transcriptomes of lowland and highland mice from in situ and F_1 groups, and associated variation in transcriptome-wide gene expression with measures of whole-organism NST performance under hypoxia using a network-based gene co-expression analysis (WGCNA; Langfelder & Horvath 2008). The results of this study provide insight into the ways in which transcriptome-wide regulatory changes can affect the evolution of complex phenotypic traits that influence fitness.

Materials and methods

Study populations and acclimation procedures

Wild-captured lowland (*Peromyscus maniculatus nebracensis*) and highland (*Peromyscus maniculatus rufinus*) deer mice were collected from two locations in central North America in August 2014: lowland mice were collected in the tallgrass prairie of eastern Nebraska (9 mile prairie; Lancaster Co., Nebraska; 40°52′12″N, 96°48′20.3″W; 430 m above sea level; PO_2 ~152 mm Hg), and highland mice were collected from the summit of Mt. Evans in the Rocky Mountains (Clear Creek Co., Colorado; 39°35′18″N, 105°38′38″W; 4350 m above sea level; PO_2 ~95.6 mm Hg). Subsets of mice from both populations were transported to the animal research facility at University of Illinois at Urbana-Champaign (Urbana, IL; elevation ~200 m), where they were crossed to produce F_1 progeny. Laboratory-reared mice were maintained at a constant ambient temperature between 20 and 22 °C, and 12-h : 12-h light : dark schedule. Mice were given food and water ad libitum. Field collecting permits for Mt. Evans were obtained from Colorado Parks and Recreation (licence no. 15TR2148) and the National Forest Service (permit no. CLC731).

We assessed nonshivering thermogenic (NST) performance and BAT transcriptional profiles of wild-captured (in situ) and the progeny of wild-captured (F_1) lowland and highland deer mice. In situ mice from lowland (n = 10) and highland (n = 6) populations were sampled at their native elevations within 1–2 days of

capture. F_1 mice were sampled once they reached adulthood (*c.* 90 days; $n = 10$ mice per population). We sampled full-sibling F_1 mice from three lowland families and two highland families. All 36 sampled mice were measured for NST performance, while a subset ($n = 19$; see below) was used in the assessment of BAT transcriptional profiles.

Measurement and analysis of nonshivering thermogenesis

We measured NST using open-flow respirometry (Cheviron *et al.* 2012) following a standard dose of CL-316,243 (hereafter CL), a selective agonist of β_3-adrenergic receptors in BAT (Bloom *et al.* 1992). Prior to CL injection, we measured oxygen consumption (VO_2) continuously for 2 h to estimate resting metabolic rate (RMR) and to establish a baseline VO_2 to detect BAT activation. During these measurements, mice were placed into a metabolic chamber (interior volume of 180 mL) and maintained at 27 °C, a temperature that is within the thermoneutral zone for *P. maniculatus* (Hayward 1965). To simulate high-elevation conditions in our in situ measurements of lowland mice and our laboratory measurements of the F_1 mice, we exposed individuals to hypoxic nitrox (12.6% O_2, balance N_2). This O_2 concentration simulates the level of hypoxia experienced on the summit of Mt. Evans (Cheviron *et al.* 2013). We maintained incurrent nitrox flow rates of 500 mL/min STPD using an FB8 Sable Systems (Las Vegas, NV) mass flow controller. For the in situ measures of mice on the summit of Mt. Evans, we used ambient air instead of nitrox, but we maintained equivalent flow rates of 500 mL/min STPD. We subsampled approximately 150 mL/min of excurrent gas (nitrox or ambient air), which was scrubbed of CO_2 and water vapour using ascarite and drierite, respectively, before being routed to the O_2 analyzer (FoxBox Sable Systems, Las Vegas, NV). We used infrared cameras (model WCM-6LNV, Sabrent) to visually monitor the mice over the course of the trial and to ensure that individuals were resting and inactive. Following this baseline RMR measurement, we injected mice with a standard intraperitoneal dose of 0.5 mg/kg of CL delivered in sterilized saline. This dose is within the range of those used to estimate NST in a variety of other small mammals (Sell *et al.* 2004; Bauwens *et al.* 2011; Müller *et al.* 2013), and our preliminary trials demonstrated that it was sufficient to induce a detectable increase in VO_2 over sham (saline) injections without inducing an undesirable increase in agitation or activity. Following the injection, we returned the mice to metabolic chambers, allowed them to recover for 30 min and then recorded VO_2 continuously for an additional 1.5 h. We calculated VO_2 using equation 10.1 in Lighton (2008) and estimated RMR as the lowest average VO_2 over continuous 10-min period. We then estimated NST as the highest 5-min continuous average VO_2 following CL injection, minus RMR, provided that the mice were known to be resting and inactive during the sampling period. All NST values were then normalized to body mass. Following the metabolic measurements, we returned mice to the colony, allowed them to recover for 2 days and euthanized them via cervical dislocation following isoflurane anaesthesia and dissected out BAT for downstream transcriptomic analysis. All experimental procedures were approved by the University of Illinois IACUC (protocol #14171).

We analysed the effects of population (highland vs. lowland), rearing group (in situ vs. F_1) and their interaction on NST values using a two-way analysis of covariance (ANCOVA) with body mass as a covariate. We measured body mass before both NST and RMR measurements, and the mean of these two body mass measurements was used as the covariate in the ANCOVA. Upon detection of significant main effects of population, we performed post hoc one-way ANCOVAs to determine whether population differences in NST were present in one or both rearing environments (in situ and F_1) while controlling for the effects of body mass on NST. ANCOVAs were performed in R version 3.2.2.

Library preparation, sequencing and read mapping

To investigate the influence of regulatory variation on population differences in NST, we performed massively parallel sequencing of brown adipose tissue (BAT) transcriptomes (RNA-seq; Wang *et al.* 2009) from 19 highland and lowland deer mice from each rearing group subjected to NST trials (In situ: highland, $n = 5$; lowland, $n = 5$; F_1: highland, $n = 4$; lowland, $n = 5$). BAT RNA was extracted prior to sequencing using TRI Reagent (Sigma-Aldrich, St. Louis, MO, USA) following the manufacturer's instructions. We generated Illumina sequencing libraries using a TruSeq RNA Sample Preparation Kit v2 (Illumina, San Diego, CA, USA). The libraries were sequenced as 100nt single-end reads on an Illumina HiSeq2500 platform with 10 individuals multiplexed per lane using Illumina index adaptors. Separate sequencing runs were conducted for in situ and F_1 mice. Raw sequences have been deposited in NCBI Sequence Read Archive (Accession no. SRP073101).

We performed a series of filtering steps to remove artefacts generated during the sequencing process. Reads with an average Phred quality score of <30 were removed from each library, after which low-quality bases were removed from the remaining high-quality

sequences (*Trim Sequences* function in CLC Genomics Workbench v6; Limit = 0.05). Adaptor sequences, if detected, were trimmed from sequence reads. Quality control steps yielded a total of almost 311 million reads with an average of 16 million reads per individual (range = 12–22 million) and an average read length of 99.1 bp.

After cleaning and trimming, sequence reads were mapped to the *Peromyscus maniculatus bairdii* genome (Pman_1.0; GenBank Accession no.: GCA_000500345.1). We then computed transcript abundance values for each gene using CLC Genomics Workbench v6. Sequence reads mapped to a total of 27 106 unique genes. Since genes with low read counts are subject to increased measurement error (Robinson & Smyth 2007), we excluded those with less than an average of five reads per individual. A total of 16 406 genes were retained after filtering.

Because the *P. maniculatus* genome is a first draft assembly, we analysed its utility as a reference by comparing our mapping and differential expression results to those obtained from using the high-quality and well-annotated *Mus musculus* genome, which has been used in previous studies assessing expression variation between lowland and highland deer mice (Cheviron *et al.* 2012, 2014; Scott *et al.* 2015). Differential expression analysis was performed in edgeR (Robinson & Oshlack 2010; Robinson *et al.* 2010) and is described in detail below. Although the *P. maniculatus* genome contains fewer annotated genes than *M. musculus*, our analysis (see Results section 'Comparative analysis of reference genomes'; Fig. 2) demonstrates that using *P. maniculatus* as a reference improves read mapping and yields quantitatively similar differential expression results compared to mapping to the *M. musculus* genome. We subsequently chose to map to *P. maniculatus* over *M. musculus* since the improved mapping rate is likely to enhance the detection of highly divergent, rapidly evolving genes. All downstream analyses were therefore performed using the *P. maniculatus* reference genome.

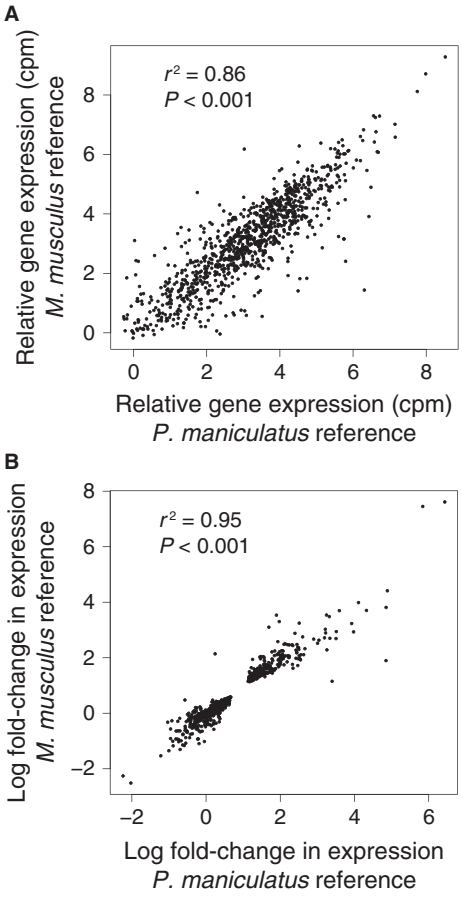

Fig. 2 Results of the comparison between *Peromyscus maniculatus* and *Mus musculus* as reference genomes in read mapping conducted in order to assess the utility of *P. maniculatus* as a reference. (A) Average relative gene expression across all populations and conditions. Values are log-transformed counts per million (cpm). Correlation analysis includes genes that passed filtration steps (see Materials and methods) for both reference genomes (n = 8372). A random subset of 1000 genes is plotted for clarity. (B) Log fold change in relative gene expression between lowland and highland populations. Genes with an uncorrected $P < 0.05$ (according to differential expression analysis; see Materials and methods) are plotted (n = 636). The use of *P. maniculatus* as a reference genome yields quantitatively similar gene expression results compared to that of *M. musculus*.

Gene co-expression network analysis and module detection

Functional analysis of suites of genes with highly correlated expression patterns can yield important insight into the mechanistic basis of complex trait variation (Ayroles *et al.* 2009; Cheviron *et al.* 2014; Scott *et al.* 2015; Stager *et al.* 2015). Weighted gene co-expression network analysis (WGCNA v. 1.41-1; Langfelder & Horvath 2008) is increasingly being used as a systems biology method for identifying clusters of highly correlated transcriptional modules and relating them to higher level phenotypic variation (Fuller *et al.* 2007; Voineagu *et al.* 2011; Filteau *et al.* 2013; Plachetzki *et al.* 2014). We used WGCNA to build an unsigned, co-expression network from read count data of BAT genes across rearing environments and populations. The co-expression network was subsequently used to identify highly correlated transcriptional modules. Prior to WGCNA, raw read counts were normalized by total library size using the function *calcNormFactors* in edgeR. The function *cpm* (edgeR) was then used to transform reads into $\log_2$ counts per million (cpm) for downstream analysis.

Network construction and module detection was performed using the *blockwiseModules* function in WGCNA with default parameters (Langfelder & Horvath 2008). Briefly, co-expression networks were created by calculating pairwise Pearson correlations between pairs of genes, after which an adjacency matrix was computed by raising the correlation matrix to a soft thresholding power of $\beta = 7$. Soft thresholding power β is chosen to achieve an approximately scale-free topology network, an approach that favours strong correlations over weak ones (Zhang & Horvath 2005). A β of seven was chosen since it represents the value for which improvement of scale-free topology model fit begins to decrease with increasing thresholding power (i.e. the inflection point; Fig. S1, Supporting information). A topological overlap measure (a robust measure of interconnectedness) was computed from the resulting adjacency matrix for each gene pair. Topological based dissimilarity was then calculated and used as input for average linkage hierarchical clustering in the creation of cluster dendrograms (Fig. S2, Supporting information). Modules (clusters of densely interconnected and highly correlated genes) were identified as branches of the resulting cluster tree using the dynamic tree-cutting method (Langfelder & Horvath 2008; Fig. S2, Supporting information).

Identification and analysis of NST-associated co-expression modules

Once transcriptional modules were defined, we used a multistep process to identify which modules were associated with variation in NST performance. First, we summarized module expression using a principal components analysis (PCA) of gene expression profiles (implemented in *blockwiseModules* function in WGCNA). Because genes within modules are highly correlated by definition, the first principal component (PC1) of a PCA on their expression can be used to represent overall module expression (Langfelder & Horvath 2008; Cheviron *et al.* 2014; Scott *et al.* 2015). PC1 values from this analysis are hereafter referred to as module eigengenes (terminology of Langfelder & Horvath 2008). We then used module eigengene values to test for associations between module expression and NST performance (Pearson correlation; *cor* function in WGCNA). *P*-values for the correlation were determined by a Student's asymptotic test using the function *corPvalueStudent* in WGCNA.

We created an interaction network among co-expression modules using Cytoscape (Cline *et al.* 2007; Smoot *et al.* 2011; Fig. 4). Network connections between modules (referred to as nodes) were computed as the pairwise Pearson correlation between module eigengenes (*corr.test* function in R). To determine whether NST-associated modules were nonrandomly distributed in the interaction network, we compared a suite of network statistics [extracted using the Network Analyzer Tool in Cytoscape (Assenov *et al.* 2008)] between NST-associated and unassociated modules using one-tailed t-tests. We tested for differences between NST-associated and unassociated modules in the following network statistics: degree (number of network connections), topological coefficient (a measure of the extent to which a node shares neighbours with other nodes) and average shortest path length (a measure of the distance between two nodes).

We then performed functional enrichment analysis on the coregulated genes within each NST-associated module in order to determine the 'biological process' Gene Ontology (GO) terms overrepresented relative to those present in the genome. Enrichment analysis was conducted using hypergeometric testing implemented in GOrilla (Eden *et al.* 2009). We next identified a set of highly connected intramodular genes (hubs; Langfelder & Horvath 2008) for each NST-associated module. Hub genes are, by definition, strongly correlated with both overall module expression and NST, and thus serve as a representative of the module. We defined a single hub gene for each module as the most highly connected gene according to an intramodular connectivity score k_{ME}, defined as the Pearson correlation between hub gene expression and module eigengene (Langfelder & Horvath 2008).

Population differences in expression of NST-associated modules

We implemented a series of tests to determine whether the expression of genes in NST-associated modules differed significantly between highland and lowland deer mice. Tests were conducted separately on in situ and F_1 mice in order to isolate the effects of population (highland vs. lowland) on variation in gene expression within rearing environments. First, we used analysis of variance (ANOVA) to test for within-condition population differences in module eigengenes. This analysis tested for overall differences in module expression. Module eigengene values were rank-transformed prior to analysis to meet the assumptions of normality. We conducted one-way ANOVAs (effect of population on module eigengene) after determining that there were no significant effects of sex or sex and family in in situ or F_1 analyses, respectively ($P > 0.05$). Raw ANOVA *P*-values were corrected for multiple testing using a false discovery rate (FDR) correction of 0.05 (Benjamini & Hochberg 1995).

We then conducted a targeted analysis of differential gene expression within NST-associated modules in

which we (i) determined the proportion of module genes that were differentially expressed and (ii) examined expression difference among hub genes for each module. Differential expression analysis was conducted on genes in the filtered BAT transcriptome using edgeR (Robinson & Oshlack 2010; Robinson *et al.* 2010). First, the function *calcNormFactors* was used to normalize read counts among all libraries, after which model dispersion for each transcript was estimated separately using the function *estimateGLMTagwiseDisp* (McCarthy *et al.* 2012). We tested for differences in transcript abundance using a generalized linear model (GLM). A single main effect (population) was included in the model. We controlled for multiple testing by enforcing a genome-wide FDR of 0.05. For tests of hub gene differential expression, raw *P*-values from the edgeR GLM were FDR-corrected ($n = 9$).

Candidate gene expression analysis

In addition to our discovery-based analysis, we tested for population differentiation in expression among candidate genes with known roles in cold-induced stimulation of NST in BAT. Figure 1 depicts a simplified diagram of the genes and processes involved. First, we performed targeted differential gene expression analysis of VEGF pathway genes, since this pathway is stimulated by norepinephrine (NE) and responsible for promoting O_2 supply to BAT (Cannon & Nedergaard 2004). Genes associated with the VEGF pathway in *Mus musculus* were obtained from the MOUSE GENOME INFORMATICS database (http://www.informatics.jax.org). Expression analysis was conducted among a suite of genes and gene families in the β_3 adrenergic signalling pathway, since it is directly responsible for the cascade of events leading to NST (Fig. 1; Cannon & Nedergaard 2004). We included genes and gene families that (i) transduce the NE signal: β_3 adrenergic receptor (*Adrb3*), adenylyl cyclase (*Adcy1*, *Adcy2*, *Adcy3*, *Adcy4*, *Adcy5*, *Adcy6*, *Adcy7*, *Adcy8*, *Adcy9*), stimulatory G protein (*Gnas*), protein kinase A subunits (*Prkaca*, *Prkacb*, *Prkar1ba*, *Prkar1b*, *Prkar2a*, *Prkar2b*); (ii) promote brown adipocyte proliferation via anti-apoptosis: src (nuclear co-activator receptor 1; *Ncoa1*), Erk1/2 (*Mapk1*, *Mapk3*); (iii) promote uncoupling protein 1 (*Ucp1*) transcription: cAMP response element binding proteins (CREB; *Creb1*, *Creb3*, *Creb5*, *Crebl1*, *Crebl2*, *Creb3l1*, *Creb3l2*, *Creb3l4*, *Creb3l5*), CCAAT enhancer binding protein (C/EBP; *Cebpa; Cebpb*); (iv) influence lipolysis and fatty acid transport: hormone sensitive lipase (*Lipe*), fatty acid binding proteins (*Fapb3*, *Fapb4*); as well as (v) *Ucp1* itself. Raw *P*-values from the edgeR GLM were FDR-corrected for multiple testing as above ($n = 35$).

Results

Measurement of nonshivering thermogenesis

The ANCOVA analysis revealed significant effects of population (highland vs. lowland; $F_{1,\ 31} = 25.96$, $P = 1.63 \times 10^{-5}$) and rearing environment (in situ vs. F_1; $F_{1,31} = 15.74$, $P = 0.0004$) on nonshivering thermogenic capacity (NST). At their native altitudes, highland and lowland deer mice differed significantly in NST, but this difference did not persist in the F_1 mice (Fig. 3). Post hoc tests revealed that highland mice exhibited significantly higher NST than lowland mice in the in situ group ($F_{1,13} = 34.27$, $P = 5.65 \times 10^{-5}$), but NST did not differ between populations in the F_1 group ($F_{1,17} = 2.75$ $P = 0.15$). For highland mice, NST remained high under both field and laboratory conditions (Fig. 3). Lowland mice exhibited greater NST in the F_1 compared to in situ condition, a result that may be accounted for by a single, full-sibling family (lowland family 48; Fig. 3); removal of lowland family 48 from the analysis results in a statistically significant effect of population in the F_1 treatment ($F_{1,13} = 8.44$, $P = 0.012$).

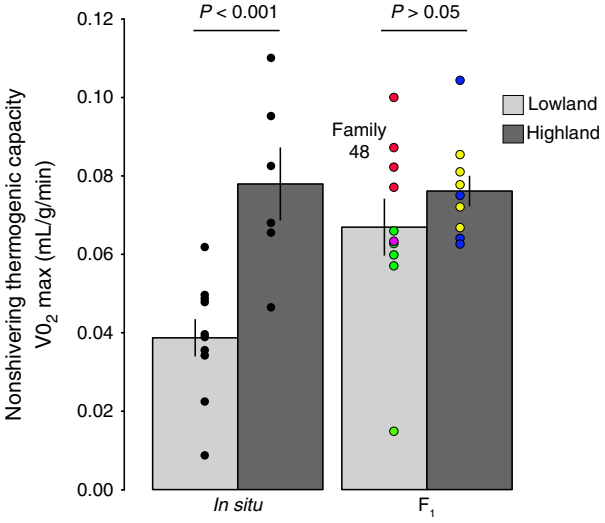

Fig. 3 Nonshivering thermogenic capacity of lowland and highland deer mice in each of two rearing groups: mice were tested at their native elevation (in situ) and in the laboratory (F_1). Bars are presented as mean ± standard error of the mean. Dots represent individuals. For F_1 mice, families are coloured as follows: red: lowland family 48; green: lowland family 25; violet: lowland family 27; blue: highland family 46; yellow: highland family 31. Family information was unavailable for in situ mice.

Comparative analysis of reference genomes

Using *Peromyscus maniculatus* as a reference genome results in an improved mapping rate, but a decreased annotation rate, compared to *Mus musculus*. Approximately 10% more sequence reads mapped to the *P. maniculatus* genome than to the *M. musculus* genome: 48.5% and 39.2%, respectively. Similarly, after filtering for low read counts, 1420 more *P. maniculatus* genes were retained compared to *M. musculus* (16 406 vs. 14 986). The use of *P. maniculatus* as a reference appears to maximize the number of genes for which expression is detectable. This result likely reflects the considerable evolutionary divergence between these species (estimated divergence time is approximately 24 mya; Steppan *et al.* 2004). Although mapability is higher when *P. maniculatus* is used, approximately 4000 genes remained unannotated in the filtered data set. To improve downstream functional analysis, we sought to identify these unannotated genes using BLAST searches against the *M. musculus* protein database (USEARCH utility; weak *E*-value = 0.0001; strong *E*-value = 1e-9). We retained the best hit for each *P. maniculatus* locus, resulting in the annotation of an additional 2815 genes. These additional gene annotations are archived in online supporting material (Table S8, Supporting information).

Computation of gene expression and differential expression analysis yielded quantitatively similar results when *P. maniculatus* or *M. musculus* reference genomes were used. Average relative gene expression (counts per million) was highly correlated among genes retained using both reference genomes ($n = 8374$; Fig. 2A). A differential expression analysis revealed that, among genes with significant population effects (P-value < 0.05; $n = 636$), log fold changes in expression were nearly identical between data sets (Fig. 2B). Thus, population differences in expression occur in the same magnitude and direction whether *P. maniculatus* or *M. musculus* is used as a reference. Overall, mapping to *P. maniculatus* provides an advantage over *M. musculus* in that an improved mapping rate may enhance the detection of genes with high levels of sequence divergence between the two species.

WGCNA and analysis of NST-associated modules

We detected 38 unique modules of putatively coregulated genes (hereafter M1–M38) based on the gene co-expression network created in WGCNA. The number of genes present in each module ranged from 41 to 2703 (Fig. 4). Module assignment of each gene used in WGCNA is available in electronic supplementary material (Table S1, Supporting information). Principal components analysis was used to summarize gene expression profiles of modules as PC1 scores (known as module eigengenes). The proportion of variance explained by PC1 ranged from 37% to 57%. An interaction network representing the relationships among the 38 co-expression modules is presented in Fig. 4. Connections between modules represent significant ($q < 0.05$) positive or negative Pearson correlations between module eigengenes.

Tests for associations between module eigengene and NST performance revealed nine modules (M5, M13, M15, M21, M23, M31, M33, M34 and M36) with significant correlations ($P < 0.05$; Fig. 4); correlation plots, correlation coefficients and P-values for each NST-associated module are presented in Fig. 5. Correlation analysis results for all other modules are available in electronic supplementary material (Table S2, Supporting information). Visual inspection of the interaction network suggested that NST-associated modules tended to occupy more peripheral and less connected positions compared to modules that are not associated with NST (Fig. 4). Network analysis in Cytoscape confirmed visual inspection: NST-associated modules have fewer network connections (associated avg. = 2.44 vs. unassociated avg. = 3.67; $P = 0.026$), share fewer network neighbours (associated avg. topological coefficient = 0.306 vs. unassociated avg. = 0.351; $P = 0.008$) and exhibit lower shortest path distances (associated avg. = 2.89 steps vs. unassociated avg. = 3.35 steps, $P = 0.007$).

Enrichment analysis identified 539 enriched GO terms ($q < 0.05$) among four of the nine NST-associated modules (M5, M23, M34, M36; Table S3, Supporting information). In particular, module M23 was enriched for several GO terms related to tissue O_2 diffusion including the terms 'angiogenesis' and 'vasculogenesis' as well as terms related to tissue growth ('tissue morphogenesis') and brown adipocyte proliferation ('Erk 1/2 cascade'; Table 1). Modules M5, M34 and M36 were significantly enriched for GO terms related to immune system processes, including the GO terms 'immune system processes' and 'immune response' (Table S3, Supporting information). No other NST-associated modules were significantly enriched for GO terms at the $q < 0.05$ level.

Population differentiation of NST-associated modules

Population differences in the expression of NST-associated modules (as measured by module eigengene) were generally more prevalent in situ than among laboratory-raised F_1 mice. Seven of the nine NST-associated modules exhibited significant population differences in situ (Table 2). Fewer modules exhibited constitutive differences in expression across both conditions (four of

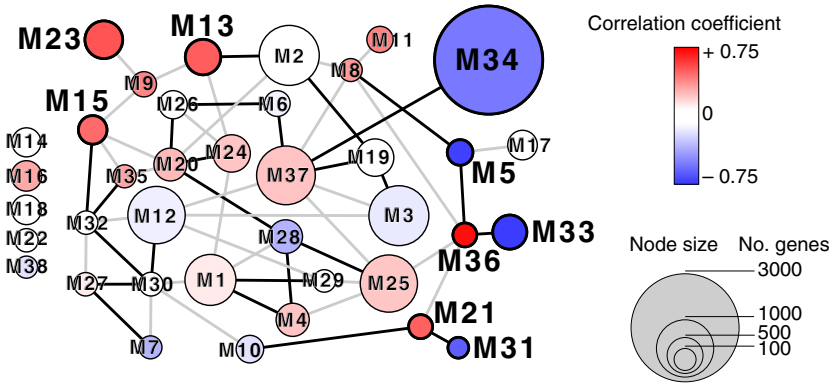

Fig. 4 Interaction network of the 38 gene co-expression modules (nodes) identified by WGCNA (Langfelder & Horvath 2008). Node size reflects the number of genes within each module. Lines connecting nodes (connections) represent significant ($q < 0.05$) positive (grey lines) or negative (black lines) pairwise correlations between modules. Node colour represents the correlation between module expression (module eigengene; see Materials and methods) and nonshivering thermogenic (NST) capacity. Red: positive correlation. Blue: negative correlation. Modules exhibiting a significant ($P < 0.05$) correlation with NST are bolded.

nine modules), and none of the modules exhibited a significant population difference within the F_1 group alone (Table 2). These patterns of population differentiation in module expression were mirrored at the level of individual module genes: for all but a single module (M21), a greater proportion of genes were differentially expressed ($q < 0.05$) between populations in situ vs. those tested in the laboratory (Table S7, Supporting

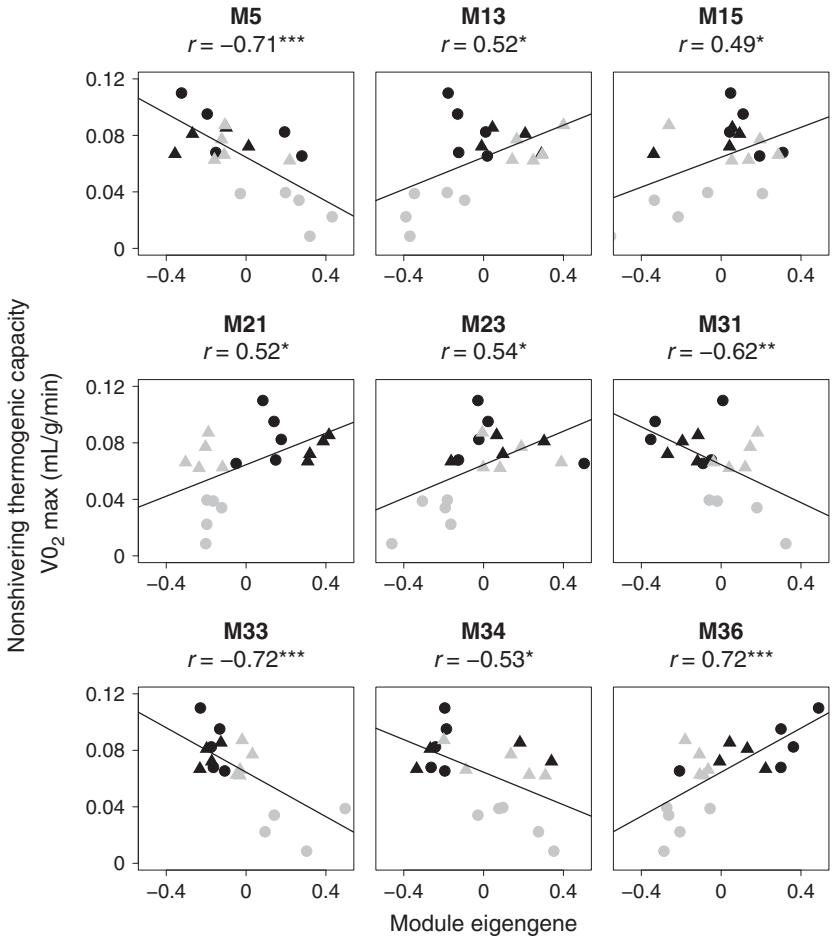

Fig. 5 Correlations between module eigengene and nonshivering thermogenic (NST) capacity of highland (black) and lowland (grey) deer mice from in situ (circles) and F_1 (triangles) conditions. Only modules with significant ($P < 0.05$) correlations are shown. $^*P < 0.05$; $^{**}P < 0.01$; $^{***}P < 0.001$; $^{\dagger}q < 0.05$. q-value represents P-value corrected for multiple testing using the FDR method (see Materials and methods).

Table 1 Selected enriched Gene Ontology (GO) terms from module M23. M23 was positively associated with NST (see Fig. 5), and expression was significantly higher among highland mice in situ (see Table 2)

GO term	Description	*P*	*q*	Enrichment	*N*	*B*	*n*	*b*
GO:0001525	Angiogenesis	2.42E-09	4.37E-06	3.67	13 408	200	511	28
GO:0048514	Blood vessel morphogenesis	8.13E-05	1.03E-02	4.01	13 408	72	511	11
GO:0007219	*Notch* signalling pathway	8.61E-05	1.07E-02	3.7	13 408	85	511	12
GO:0043547	Positive regulation of GTPase activity	4.66E-07	2.19E-04	2.76	13 408	285	511	30
GO:1904018	Positive regulation of vasculature development	1.05E-04	1.27E-02	3.41	13 408	100	511	13
GO:0045765	Regulation of angiogenesis	1.25E-07	8.31E-05	3.68	13 408	157	511	22
GO:0070372	Regulation of ERK1 and ERK2 cascade	6.79E-05	9.15E-03	2.93	13 408	152	511	17
GO:0048729	Tissue morphogenesis	2.94E-07	1.69E-04	2.82	13 408	279	511	30
GO:0001570	Vasculogenesis	4.13E-04	3.74E-02	3.94	13 408	60	511	9

Tests were implemented in GOrilla (Eden *et al.* 2009). Enrichment scores were calculated as follows: $(b/n)/(B/N)$, where N = the total number of terms in the filtered BAT transcriptome, B = the number of terms associated with each GO term, n = the total number of genes in module, b = the number of genes associated with each GO term within each module. An enrichment score of 1.0 indicates that the proportion of terms in the module and reference genome is equivalent. See Table S3 for all enriched GO terms in this module. *q*-value represents *P*-value corrected for multiple testing using the FDR method (see Materials and methods).

Table 2 Results of ANOVA testing for population differences in module expression (represented as the module eigengene; see Materials and methods) among NST-associated modules. Tests were conducted separately for each rearing environment (in situ and F_1) to isolate the effects of population (highland vs. lowland) on variation in gene expression within rearing environments

Module	No. of genes	In situ			F_1		
		$F_{(1,8)}$	*P*	*q*	$F_{(1,8)}$	*P*	*q*
M5	188	4.3	0.07	0.07	0.2	0.70	0.74
M13	489	6.2	0.04	**0.05**	1.6	0.24	0.37
M15	279	4.3	0.07	0.07	1.6	0.24	0.37
M21	139	25.0	0.001	**0.002**	21.0	0.003	**0.006**
M23	558	25.0	0.001	**0.002**	0.1	0.83	0.83
M31	41	6.2	0.04	**0.05**	21.0	0.003	**0.006**
M33	447	25.0	0.001	**0.002**	21.0	0.003	**0.006**
M34	2703	25.0	0.001	**0.002**	0.2	0.66	0.74
M36	136	9.2	0.02	**0.03**	21.0	0.003	**0.006**

q-Value represents *P*-value corrected for multiple testing using the FDR method (see Materials and methods). Bold values indicate $q < 0.05$.

information). This pattern was also detected across the BAT transcriptome as a whole: although transcriptome-wide population differences in gene expression ($q < 0.05$) were detected under both rearing conditions, four times as many genes were differentially expressed in in situ vs. F_1 mice, and only a small proportion (81 genes) of genes were population-differentiated under both rearing conditions (Fig. S3, Supporting information).

We subsequently tested for population differences in expression of hub genes within each NST-associated module; since hubs are highly correlated with overall module expression, and hence other genes in the module, they are likely to represent key genes in the regulation of module pathways (Langfelder & Horvath 2008). Hub genes from seven of nine NST-associated modules were significantly differentiated ($q < 0.05$) between highland and lowland populations in situ (Fig. 6; Table S4, Supporting information). Expression of two hub genes remained significantly differentiated between populations in the F_1 treatment: *Atp11b* (ATPase, class VI, type 11B; M21) and *Hba-a1* (α haemoglobin; M31).

Candidate gene expression analysis

Nine a priori defined candidate genes exhibited significant population differences in expression (Fig. 7). These genes play known roles in the β3 adrenergic receptor signalling cascade, the transcription of *Ucp1* and lipolysis, all of which facilitate NST within brown adipocytes (see Fig. 1). The majority of genes were upregulated in highland compared to lowland mice in situ ($q < 0.05$; Fig. 7). No candidate genes were differentially expressed between F_1 treatment mice ($q > 0.05$). Although *Ucp1* expression was 1.5× greater in in situ highland compared to lowland mice, this difference did not reach statistical significance ($P = 0.08$; $q = 0.35$). Results of analysis for all candidate genes are reported in Table S5 (Supporting information).

Discussion

The cold and hypoxic conditions of high altitude have resulted in strong selection for the enhancement of aerobic thermogenic heat production in deer mice (Hayes & O'Connor 1999). Adaptations of the skeletal

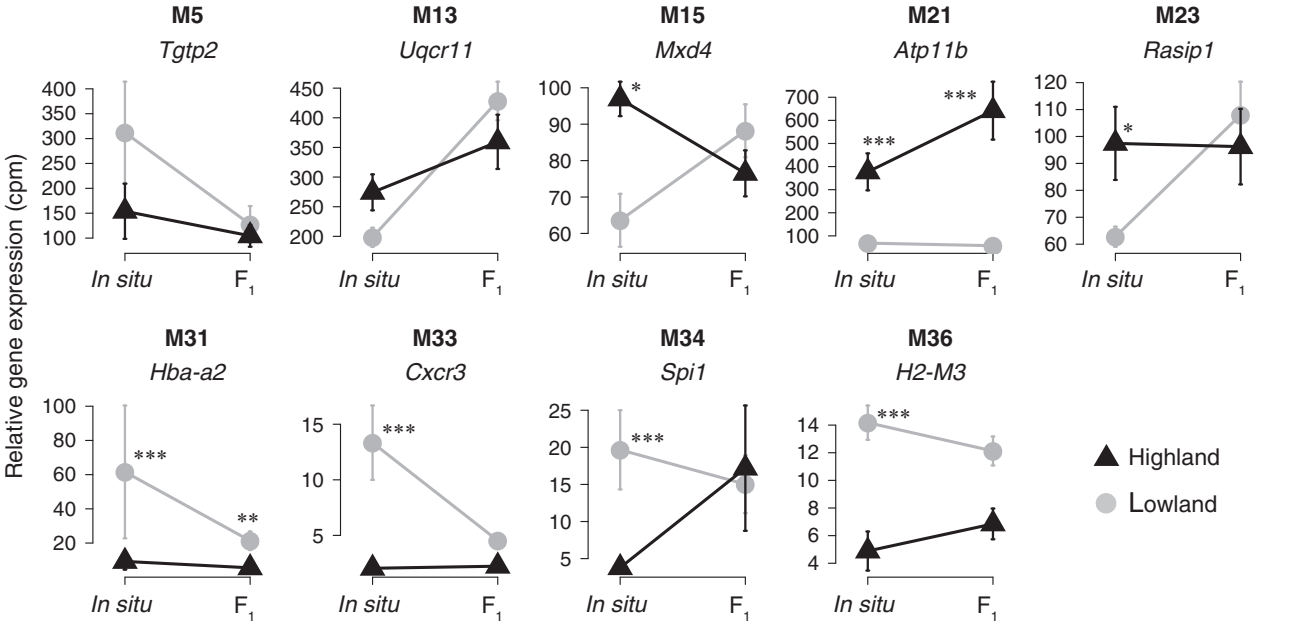

Fig. 6 Plots of hub gene expression among highland (dark triangles) and lowland (light circles) deer mice from in situ and F_1 rearing environments. The name of each hub gene is listed below the module from which it is derived. Values are mean counts per million (cpm) ± standard error of the mean. *$q < 0.05$; **$q < 0.01$; ***$q < 0.001$ according to results of a GLM testing for population differences in transcript abundance within each rearing environment. Exact *P*- and *q*-values reported in Table S4. *q*-Value represents *P*-value corrected for multiple testing using the FDR method (see Materials and methods).

musculature and regulatory networks that participate in shivering thermogenesis partially explain adaptive increases in whole-organism thermogenic capacity under hypoxia (Cheviron *et al.* 2012, 2013, 2014; Lui *et al.* 2015; Scott *et al.* 2015). However, because deer mice rely heavily on nonshivering mechanisms for cold acclimatization (Van Sant & Hammond 2008), we tested for evidence of population divergence in nonshivering thermogenesis (NST) under hypoxia to compliment earlier studies of muscle phenotype. Our results suggest that adaptation to severe hypoxic cold stress is influenced by plastic increases in NST. This plasticity appears to be mediated by the upregulation of genes that influence several intersecting physiological pathways within BAT, including the supply of O_2 to the tissue, the growth and differentiation of brown adipocytes and a suite of genes that facilitate cellular uncoupling of oxidative phosphorylation from ATP synthesis in the generation of heat.

Population differences in nonshivering thermogenesis under hypoxia

When measured at their native altitudes, NST was twofold higher in highland compared to lowland deer mice, although these differences did not persist in comparisons of F_1 mice that were born and reared in common garden, low-elevation conditions (Fig. 3). This suggests that population differences in NST that are present in mice acclimatized to their native altitudes are the result of phenotypic plasticity. This increased capacity for NST is associated with greater total thermogenic capacity under hypoxia (Cheviron *et al.* 2012, 2013), a trait under strong directional selection in highland deer mice (Hayes & O'Connor 1999). These results suggest that plasticity in NST is adaptive in that it contributes to an enhanced thermogenic performance at high altitude (e.g. Ghalambor *et al.* 2007).

Under laboratory conditions, F_1 deer mice from both populations exhibited equivalent and elevated NST (Fig. 3). This result probably reflects the fact that mice were reared at a temperature (20–22 °C) below thermoneutrality (approximately 27 °C for deer mice; Hayward 1965). Lowland mice exhibited higher NST in the F_1 compared to the in situ condition (Fig. 3), most likely because summer temperatures in Nebraska are warmer (mean temperature for July 2015 = 25 °C; National Weather Service) than the laboratory. That highland mice exhibited no difference in NST across in situ and F_1 conditions suggests that they were acclimatized to the cold in both environments.

Lack of population differences under common, low-altitude conditions suggests that enhancement of NST capacity in high-altitude mice does not have a constitutive genetic basis. Indeed, enhanced NST among highlanders is likely to be the result of acclimatization to

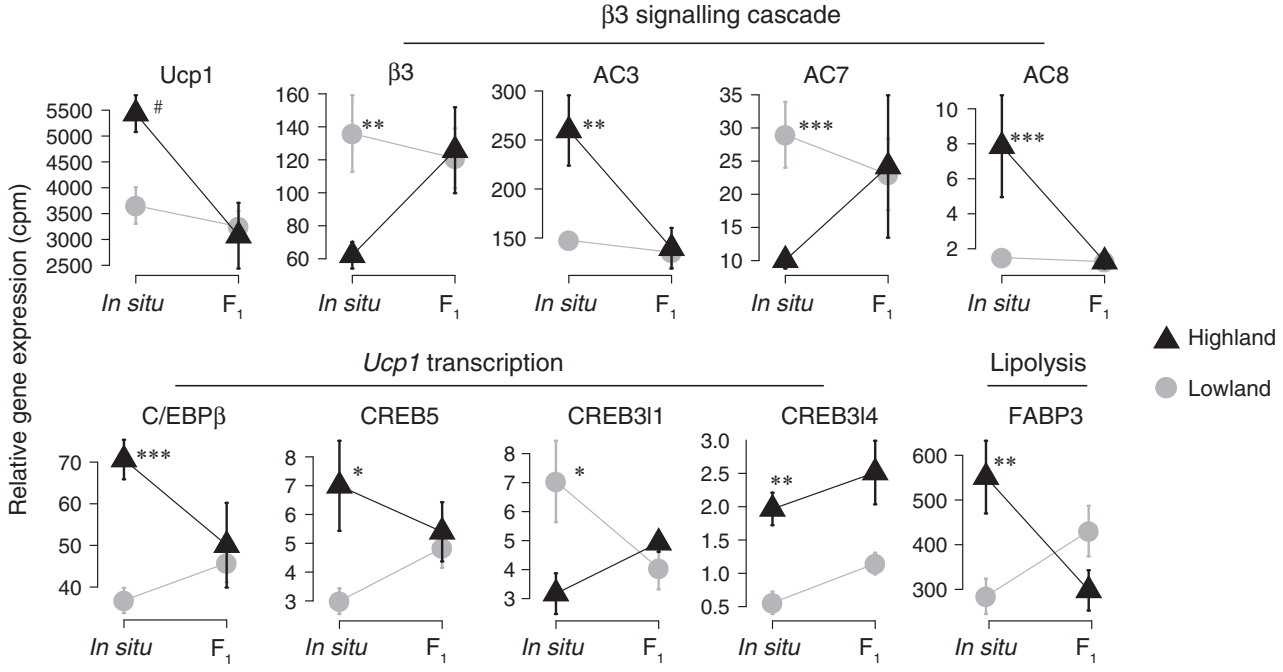

Fig. 7 Plots of candidate gene expression among highland (dark triangles) and lowland (light circles) deer mice from in situ and F_1 rearing environments. Gene names are listed and categorized in accordance with Fig. 1. Values are mean counts per million (cpm) ± standard error of the mean. *$q < 0.05$; **$q < 0.01$; ***$q < 0.001$ according to a GLM testing for population differences in transcript abundance within each rearing environment. No statistically significant ($q < 0.05$) population effects were found among F_1 mice. Exact *P*-values and *q*-values are reported in Table S5. *q*-value represents *P*-value corrected for multiple testing using the FDR method (see Materials and methods).

lower minimum temperatures experienced at high altitude. However, the lack of persistent population effects across rearing environments may be attributable to a single lowland family exhibiting high NST performance (family 48; Fig. 3); removal of family 48 from the analysis resulted in a statistically significant population effect in the F_1 group ($P < 0.05$). We cannot, however, make a conclusive inference regarding the effect of family 48 on patterns of population differentiation in NST. Future work that samples across multiple low-elevation families is needed to determine the extent of genetic variation in NST performance.

Enhanced NST among highland deer mice is present under conditions of severe O_2 deprivation, a condition that imposes well-documented constraints on aerobic performance (Hayes & Chappell 1986; Ward *et al.* 1989; Chappell & Hammond 2003). In particular, hypoxic stress is known to inhibit NST among low-altitude adapted house mice (*Mus musculus*), a condition caused by a reduction in BAT sympathetic nerve activity (a response that restricts O_2 consumption to only vital processes; Madden & Morrison 2005). Acclimation to hypoxic cold stress in house mice results in NST levels that are lower than when animals are exposed to cold alone and that are comparable to mice acclimated to normoxia at room temperature (Beaudry & McClelland 2010). Thus, in animals not specifically adapted to environmental hypoxia, the inhibitory effect of hypoxia on BAT may limit the cold-induced upregulation of NST present under normoxia. Our results suggest that highland mice may have overcome hypoxia-induced constraints on BAT function, a phenomenon that could be facilitated by any number of functional changes that enhance O_2 supply to – or O_2 utilization by – BAT. Laboratory experiments in which highland and lowland animals are cold-acclimated under normoxia or hypoxia are needed to test whether the capacity to upregulate NST under hypoxia is enhanced in high-altitude mice.

Transcriptional basis of variation in nonshivering thermogenesis

Within the BAT transcriptome, we identified modules of highly correlated, co-expressed genes, representing a set of putative regulatory networks (Langfelder & Horvath 2008; Fig. 4). We correlated the expression of these modules with variation in NST performance in order to determine which modules, if any, contributed to population differences in NST; nine modules were significantly associated with NST across deer mouse populations and experimental conditions (Fig. 5). A rank-transformed ANOVA performed on module

expression (module eigengene) revealed that the majority (seven of nine) of NST-associated modules exhibited significant expression differences between high- and low-altitude populations when measured in situ (Table 2). By contrast, population differences in module expression persisted in F_1 mice in only four of the modules (Table 2). Thus, although a few modules appear to be constitutively differentiated between lowland and highland deer mice, the majority of modules respond plastically to differences in the environment.

Consistent with this conclusion, a greater proportion of genes comprising NST-associated modules were differentially expressed between populations in situ compared to those raised in the laboratory (with the exception of M21; Table S7, Supporting information). Moreover, population differences in gene expression across all genes in the BAT transcriptome were fourfold higher in the wild than they were in the laboratory (Fig. S3, Supporting information); over 1300 genes were differentially expressed between lowland and highland mice in situ (Fig. S3, Supporting information), representing about 8% of the BAT transcriptome. These differences in gene expression are consistent with the patterns of differentiation in NST (Fig. 3) and module expression (Table 2), suggesting that acclimatization to cold hypoxia results in the differential regulation of many genes and regulatory networks across the BAT transcriptome.

Analysis of the interaction network of co-expression modules revealed that NST-associated modules occur more peripherally than unassociated modules (Fig. 4); NST-associated modules had fewer network connections, share fewer neighbours and have lower shortest path distances. That several peripherally located and NST-associated modules exhibit evolved differences in expression between high- and low-altitude deer mice is consistent with theory suggesting that loosely connected network elements may be more likely to evolve than highly connected elements. For example, mutations in highly connected genes or modules, which by definition have multiple inputs and pleiotropic effects, are more likely to result in functional alteration of other genes or pathways in the network (Davidson & Erwin 2006; Erwin & Davidson 2009). Thus, the greater potential for negative pleiotropy among highly connected genes should constrain their evolution within a network. Analysis of laboratory-reared deer mice exposed to a range of O_2 tensions and temperatures will further illuminate whether highly connected modules are constrained by negative pleiotropy.

Functional enrichment analysis identified several NST-associated modules that were enriched for pathways that are likely to contribute to the observed enhancement of NST among highland mice. One module in particular, M23, was functionally enriched for genes involved in O_2 supply to BAT and the proliferation of brown adipocytes (Table 1). Significantly enriched GO terms included angiogenesis, vasculogenesis, *Notch* signalling, tissue morphogenesis and regulation of the Erk 1/2 cascade (Table 1). Erk 1/2 cascade is an important component of brown adipocyte proliferation, since it facilitates the inhibition of apoptosis (Lindquist & Rehnmark 1998; Cannon & Nedergaard 2011; Fig. 1). The hub gene for M23 (Ras interacting protein 1; *Rasip1;* Fig. 6) is a critical component of the signalling process that leads to blood vessel formation via GTPase signalling (Xu *et al.* 2011); the GO term 'regulation of GTPase activity' is also enriched in M23 (Table 1). Furthermore, we identified expression of several additional genes in the VEGF pathway to be more highly expressed ($q < 0.05$) in highland mice in situ, including *Hras*, *Kdr* and *Pla2g4a* (3 of 28 VEGF pathways genes; Table S6, Supporting information).

Population differences in M23 expression mirror differences in NST, suggesting that the regulation of genes in this module contributes to an enhanced NST capacity in deer mice. Several lines of evidence support this conclusion. First, variation in M23 expression is strongly and positively correlated with variation in NST; while highland mice exhibit consistently high values across conditions, values for lowland mice are low in situ and upregulated in the laboratory (Fig. 5). This pattern was also detected in M23's hub gene, *Rasip1* (see Fig. 3 and *Rasip1* plot in Fig. 6). Moreover, no significant population differences in module (Table 2), hub (Fig. 6) or VEGF pathway (Table S6, Supporting information) expression were found in F_1 mice, indicating that, like NST, differentiation of M23 is the result of acclimatization to high altitude. Together, expression and functional enrichment analyses suggest that enhanced NST among highland mice is facilitated by upregulation of genes that influence O_2 and fuel delivery to BAT, the proliferation of brown adipocytes and the morphogenesis of BAT itself.

Previous work in highland deer mice has demonstrated that enhanced thermogenic performance among highlanders was associated with enhanced transcription of angiogenesis pathways in skeletal muscle (Cheviron *et al.* 2014). Moreover, Scott *et al.* (2015) found higher expression of a *Notch* gene (*Notch-4*) in muscle in highland compared to lowland deer mice subject to cold, hypoxic stress, an upregulation that is persistent in mice that were born and reared under low-altitude conditions. This greater *Notch-4* expression is associated with a highly oxidative and capillarized muscle phenotype among highlanders (Scott *et al.* 2015). Notch signalling is critical for the development of stable and patent blood vessel formation during angiogenesis

(Sainson & Harris 2008; Lv *et al.* 2013). These results suggest that regulatory changes to pathways that influence O_2 supply via vascularization of two major thermogenic organs underlie adaptive enhancement of thermogenesis among high-altitude deer mice. Regulatory changes to O_2 supply pathways are consistent with research demonstrating that high-altitude deer mice have evolved an elevated haemoglobin–O_2 affinity, which helps to maintain tissue O_2 delivery in face of severe hypoxia (Storz *et al.* 2009, 2010a; Natarajan *et al.* 2015).

We found three of the nine NST-associated modules (M5, M33, M34) to be enriched for immune system-related functions, including the GO terms 'response to interferon beta', 'immune system process', 'immune system response' and 'regulation of leucocyte activation', among many others (Table S3, Supporting information). Transcription of these immune-related modules appears to be downregulated among highland mice. These modules were negatively associated with NST (Fig. 5), and their hub genes (*Tgtp2, Cxcr3, Spi1*, respectively) exhibited lower expression compared to lowland mice (Fig. 6). Enrichment of immune-related GO terms is not likely to reflect differentiation in immune function per se, but instead is likely to be driven by differential transcription of cytokine genes that play a functional role in increasing NST capacity (Cannon *et al.* 1998). In particular, interleukin-6 (a cytokine) has been shown to stimulate NST (Busbridge *et al.* 1989; Cannon *et al.* 1998) in part by inducing *Ucp1* transcription (Li *et al.* 2002). Several interleukin genes, including the interleukin-6 receptor (*Il6r*), are associated with modules M33 and M34.

For highlanders measured in situ, decreased transcription of cytokine genes may reflect an already enhanced capacity for NST (Fig. 3), such that there is negative feedback on the expression of genes upstream of *Ucp1* expression and stimulation of NST. Indeed, transcription of β_3 adrenergic receptor (*Adrb3*) – stimulation of which signals heat generation via UCP1 (Cannon & Nedergaard 2004) – was significantly reduced among highland compared to lowland mice (Fig. 7). Such an effect is likely to be the result of acclimatization-induced stimulation of BAT in the cold conditions of high altitude. This hypothesis is supported by the fact that F_1 mice, which are acclimated to low-elevation conditions, do not exhibit differential expression of the 'immune response' module or any genes directly involved in uncoupling capacity.

Within brown adipocytes, uncoupling of oxidative phosphorylation from ATP synthesis via UCP1 is responsible for the generation of heat and is stimulated by cold-induced increases in norepinephrine (NE; Cannon & Nedergaard 2004; Fig. 1). We detected a general pattern of upregulation in genes that mediate uncoupling capacity among highland mice measured in their native environment. In particular, expression of *Ucp1* itself was 1.5-fold higher in highland mice in situ, although this result did not reach statistical significance ($q > 0.05$; Fig. 7). Since the capacity for NST is influenced by the availability of UCP1 (Cannon & Nedergaard 2004), it is likely that its upregulation is partially responsible for enhanced NST capacity in highland mice. Accordingly, we found greater transcript abundances among highland mice for several transcription factors that promote upregulation of *Ucp1* gene expression (C/EBPβ, CREB5, CREB3l1, CREB3l4; Fig. 7). Upregulation of adenylyl cyclase genes (AC3 and AC8; although AC7 exhibited the opposite pattern; Fig. 7) further suggests an enhancement in uncoupling capacity, since these genes help to transduce the NE signal that leads to upregulation of *Ucp1* and the release of free fatty acids (the substrate for thermogenesis; Cannon & Nedergaard 2004). Consistent with this result, highland mice exhibited greater transcript abundances of fatty acid binding protein (FABP3; Fig. 7), which serves as a transporter of free fatty acids (Fig. 1). Taken together, these results suggest that enhanced NST capacity under hypoxia among high-altitude mice is mediated by an increase in the transcription of genes that regulate uncoupling capacity via NE-stimulated β3 adrenergic receptor signalling.

Conclusions

For high-altitude deer mice, environmentally induced increases in NST performance appear to enhance aerobic thermogenesis under hypoxia. For mammals, the capacity for NST is determined by factors at several levels of biological organization, including vascularization of BAT (i.e. O_2 and fuel supply), the number of brown adipocytes and the availability of UCP1 (Cannon & Nedergaard 2004). We found that enhanced NST under hypoxia in highland deer mice is associated with increases in genes and transcriptional modules that influence each of these factors. Thus, under hypoxia, high-altitude deer mice appear to sustain high thermogenic capacities by up-regulating genes that facilitate high NST performance. Few genes or transcriptional modules, however, remained upregulated in laboratory-reared mice, suggesting that these traits have not been genetically canalized.

We suggest that constitutive genetic differentiation in high-altitude mice may occur primarily at steps in the O_2 cascade that influence convective O_2 transport. For example, an abundance of research has demonstrated evolution of a high O_2 affinity haemoglobin among highland mice (Snyder 1981; Snyder *et al.* 1982; Chappell & Snyder 1984; Chappell *et al.* 1988; Storz 2007;

Storz *et al.* 2007, 2009, 2010a). By contrast, changes in downstream steps of the O_2 cascade may be characterized by a higher degree of phenotypic plasticity (Cheviron *et al.* 2012, 2013, 2014; this study). This large and growing body of work suggests that both phenotypic plasticity and constitutive genetic mechanisms make important contributions to adaptive differences in thermogenic capacity between high- and low-altitude populations.

Acknowledgements

The authors would like to thank Annika Clemente, Sajeni Mahalingam, Andre Schultz and Jay Storz for assistance with fieldwork, and Elizabeth Hogan for assistance in the laboratory. Thank you to Jay Storz, Graham Scott, Grant McClelland, Phred Benham, Nicholas Sly, Maria Stager and two anonymous reviewers for helpful comments on earlier versions of this manuscript. This work was funded by grants to Z.A.C. from the National Science Foundation (IOS-1354934 and IOS-1444161).

References

Assenov Y, Ramírez F, Schelhorn S-E, Lengauer T, Albrecht M (2008) Computing topological parameters of biological networks. *Bioinformatics*, **24**, 282–284.

Ayroles JF, Carbone MA, Stone EA *et al.* (2009) Systems genetics of complex traits in Drosophila melanogaster. *Nature Genetics*, **41**, 299–307.

Bauwens JD, Schmuck EG, Lindholm CR *et al.* (2011) Cold tolerance, cold-induced hyperphagia, and nonshivering thermogenesis are normal in α_1-AMPK-/- mice. *American Journal of Physiology. Regulatory, Integrative and Comparative Physiology*, **301**, R473–R483.

Beall CM (2000) Tibetan and Andean patterns of adaptation to high-altitude hypoxia. *Human Biology*, **72**, 201–228.

Beall CM (2007) Two routes to functional adaptation: Tibetan and Andean high-altitude natives. *Proceedings of the National Academy of Sciences of the United States of America*, **104**, 8655–8660.

Beaudry JL, McClelland GB (2010) Thermogenesis in CD-1 mice after combined chronic hypoxia and cold acclimation. *Comparative Biochemistry and Physiology Part B: Biochemistry and Molecular Biology*, **157**, 301–309.

Benjamini Y, Hochberg Y (1995) Controlling the false discovery rate: a practical and powerful approach to multiple testing. *Journal of the Royal Statistical Society. Series B (Methodological)*, **57**, 289–300.

Bloom JD, Dutia MD, Johnson BD *et al.* (1992) Disodium (R, R)-5-[2-[[2-(3-chlorophenyl)-2-hydroxyethyl]amino]propyl]-1,3-benzodioxole-2,2-dicarboxylate (CL 316,243). A potent.-beta.-adrenergic agonist virtually specific for.beta.3 receptors. A promising antidiabetic and antiobesity agent. *Journal of Medicinal Chemistry*, **35**, 3081–3084.

Busbridge J, Dascombe MJ, Hoopkins S, Rothwell NJ (1989) Acute central effects of interleukin-6 on body temperature, thermogenesis and food intake in the rat. *Proceedings of the Nutrition Society*, **48**, 48A.

Cannon B, Nedergaard J (2004) Brown adipose tissue: function and physiological significance. *Physiological Reviews*, **84**, 277–359.

Cannon B, Nedergaard J (2011) Nonshivering thermogenesis and its adequate measurement in metabolic studies. *The Journal of Experimental Biology*, **214**, 242–253.

Cannon B, Houstek J, Nedergaard J (1998) Brown adipose tissue: more than an effector of thermogenesis? *Annals of the New York Academy of Sciences*, **856**, 171–187.

Chappell MA, Hammond KA (2003) Maximal aerobic performance of deer mice in combined cold and exercise challenges. *Journal of Comparative Physiology B*, **174**, 41–48.

Chappell MA, Snyder LR (1984) Biochemical and physiological correlates of deer mouse alpha-chain hemoglobin polymorphisms. *Proceedings of the National Academy of Sciences of the United States of America*, **81**, 5484–5488.

Chappell MA, Hayes JP, Snyder LRG (1988) Hemoglobin polymorphisms in deer mice (*Peromyscus maniculatus*): physiology of beta-globin variants and alpha-globin recombinants. *Evolution*, **42**, 681–688.

Chappell MA, Hammond KA, Cardullo RA *et al.* (2007) Deer mouse aerobic performance across altitudes: effects of developmental history and temperature acclimation. *Physiological and Biochemical Zoology*, **80**, 652–662.

Cheviron ZA, Brumfield RT (2012) Genomic insights into adaptation to high-altitude environments. *Heredity*, **108**, 354–361.

Cheviron ZA, Bachman GC, Connaty AD, McClelland GB, Storz JF (2012) Regulatory changes contribute to the adaptive enhancement of thermogenic capacity in high-altitude deer mice. *Proceedings of the National Academy of Sciences of the United States of America*, **109**, 8635–8640.

Cheviron ZA, Bachman GC, Storz JF (2013) Contributions of phenotypic plasticity to differences in thermogenic performance between highland and lowland deer mice. *The Journal of Experimental Biology*, **216**, 1160–1166.

Cheviron ZA, Connaty AD, McClelland GB, Storz JF (2014) Functional genomics of adaptation to hypoxic cold-stress in high-altitude deer mice: transcriptomic plasticity and thermogenic performance. *Evolution*, **68**, 48–62.

Cline MS, Smoot M, Cerami E *et al.* (2007) Integration of biological networks and gene expression data using Cytoscape. *Nature Protocols*, **2**, 2366–2382.

Conley KE, Porter WP (1986) Heat loss from deer mice (*Peromyscus*): evaluation of seasonal limits to thermoregulation. *Journal of Experimental Biology*, **126**, 249–269.

Dalziel AC, Rogers SM, Schulte PM (2009) Linking genotypes to phenotypes and fitness: how mechanistic biology can inform molecular ecology. *Molecular Ecology*, **18**, 4997–5017.

Davidson EH, Erwin DH (2006) Gene regulatory networks and the evolution of animal body plans. *Science*, **311**, 796–800.

Eden E, Navon R, Steinfeld I, Lipson D, Yakhini Z (2009) GOrilla: a tool for discovery and visualization of enriched GO terms in ranked gene lists. *BMC Bioinformatics*, **10**, 48.

Erwin DH, Davidson EH (2009) The evolution of hierarchical gene regulatory networks. *Nature Reviews Genetics*, **10**, 141–148.

Filteau M, Pavey SA, St-Cyr J, Bernatchez L (2013) Gene coexpression networks reveal key drivers of phenotypic divergence in lake whitefish. *Molecular Biology and Evolution*, **30**, 1384–1396.

Fuller TF, Ghazalpour A, Aten JE *et al.* (2007) Weighted gene coexpression network analysis strategies applied to mouse weight. *Mammalian Genome*, **18**, 463–472.

Garland T, Carter PA (1994) Evolutionary physiology. *Annual Review of Physiology*, **56**, 579–621.

Ghalambor CK, McKAY JK, Carroll SP, Reznick DN (2007) Adaptive versus non-adaptive phenotypic plasticity and the potential for contemporary adaptation in new environments. *Functional Ecology*, **21**, 394–407.

Hammond KA, Chappell MA, Kristan DM (2002) Developmental plasticity in aerobic performance in deer mice (*Peromyscus maniculatus*). *Comparative Biochemistry and Physiology Part A: Molecular & Integrative Physiology*, **133**, 213–224.

Hayes JP (1989) Field and maximal metabolic rates of deer mice (*Peromyscus maniculatus*) at low and high altitudes. *Physiological Zoology*, **62**, 732–744.

Hayes JP, Chappell MA (1986) Effects of cold acclimation on maximum oxygen consumption during cold exposure and treadmill exercise in deer mice, *Peromyscus maniculatus*. *Physiological Zoology*, **59**, 473–481.

Hayes JP, O'Connor CS (1999) Natural selection on thermogenic capacity of high-altitude deer mice. *Evolution*, **53**, 1280–1287.

Hayward JS (1965) Metabolic rate and its temperature-adaptive significance in six geographic races of *Peromyscus*. *Canadian Journal of Zoology*, **43**, 309–323.

Heldmaier G, Klaus S, Wiesinger H, Friedrichs U, Wenzel M (1989) Cold acclimation and thermogenesis. In: *Living in the Cold II* (eds Malan A, Canguilhem B), pp. 347–356. Colloque INSERM, Le Hohwald, France.

Himms-Hagen J (1985) Brown adipose tissue metabolism and thermogenesis. *Annual Review of Nutrition*, **5**, 69–94.

Janský L (1973) Non-shivering thermogenesis and its thermoregulatory significance. *Biological Reviews*, **48**, 85–132.

Langfelder P, Horvath S (2008) WGCNA: an R package for weighted correlation network analysis. *BMC Bioinformatics*, **9**, 559.

Li G, Klein RL, Matheny M *et al.* (2002) Induction of uncoupling protein 1 by central interleukin-6 gene delivery is dependent on sympathetic innervation of brown adipose tissue and underlies one mechanism of body weight reduction in rats. *Neuroscience*, **115**, 879–889.

Lighton JRB (2008) *Measuring Metabolic Rates: A Manual for Scientists: A Manual for Scientists*. Oxford University Press, New York, NY, USA.

Lindquist JM, Rehnmark S (1998) Ambient temperature regulation of apoptosis in brown adipose tissue Erk1/2 promotes norepineprhine-dependent cell survival. *Journal of Biological Chemistry*, **273**, 30147–30156.

Lui MA, Mahalingam S, Patel P *et al.* (2015) High-altitude ancestry and hypoxia acclimation have distinct effects on exercise capacity and muscle phenotype in deer mice. *American Journal of Physiology - Regulatory, Integrative and Comparative Physiology*, **308**, R779–R791.

Lv S, Cheng G, Zhou Y, Xu G (2013) Thymosin beta4 induces angiogenesis through Notch signaling in endothelial cells. *Molecular and Cellular Biochemistry*, **381**, 283–290.

Madden CJ, Morrison SF (2005) Hypoxic activation of arterial chemoreceptors inhibits sympathetic outflow to brown adipose tissue in rats. *The Journal of Physiology*, **566**, 559–573.

McCarthy DJ, Chen Y, Smyth GK (2012) Differential expression analysis of multifactor RNA-Seq experiments with respect to biological variation. *Nucleic Acids Research*, **40**, 4288–4297.

Müller TD, Lee SJ, Jastroch M *et al.* (2013) p62 links β-adrenergic input to mitochondrial function and thermogenesis. *The Journal of Clinical Investigation*, **123**, 469–478.

Natarajan C, Hoffmann FG, Lanier HC *et al.* (2015) Intraspecific polymorphism, interspecific divergence, and the origins of function-altering mutations in deer mouse hemoglobin. *Molecular Biology and Evolution*, **32**, 978–997.

Nedergaard J, Golozoubova V, Matthias A *et al.* (2001) UCP1: the only protein able to mediate adaptive non-shivering thermogenesis and metabolic inefficiency. *Biochimica et Biophysica Acta (BBA) - Bioenergetics*, **1504**, 82–106.

Plachetzki DC, Pankey MS, Johnson BR *et al.* (2014) Gene co-expression modules underlying polymorphic and monomorphic zooids in the colonial hydrozoan, *Hydractinia symbiolongicarpus*. *Integrative and Comparative Biology*, **54**, 276–283.

Robinson M, Oshlack A (2010) A scaling normalization method for differential expression analysis of RNA-seq data. *Genome Biology*, **11**, R25.

Robinson MD, Smyth GK (2007) Moderated statistical tests for assessing differences in tag abundance. *Bioinformatics*, **23**, 2881–2887.

Robinson MD, McCarthy DJ, Smyth GK (2010) edgeR: a Bioconductor package for differential expression analysis of digital gene expression data. *Bioinformatics*, **26**, 139–140.

Rosenmann M, Morrison P (1974) Maximum oxygen consumption and heat loss facilitation in small homeotherms by He-O2. *The American Journal of Physiology*, **226**, 490–495.

Sainson RCA, Harris AL (2008) Regulation of angiogenesis by homotypic and heterotypic notch signalling in endothelial cells and pericytes: from basic research to potential therapies. *Angiogenesis*, **11**, 41–51.

Scott GR, Elogio TS, Lui MA, Storz JF, Cheviron ZA (2015) Adaptive modifications of muscle phenotype in high-altitude deer mice are associated with evolved changes in gene regulation. *Molecular Biology and Evolution*, **32**, 1962–1976.

Sell H, Berger JP, Samson P *et al.* (2004) Peroxisome proliferator-activated receptor gamma agonism increases the capacity for sympathetically mediated thermogenesis in lean and ob/ob mice. *Endocrinology*, **145**, 3925–3934.

Smoot ME, Ono K, Ruscheinski J, Wang P-L, Ideker T (2011) Cytoscape 2.8: new features for data integration and network visualization. *Bioinformatics*, **27**, 431–432.

Snyder LRG (1981) Deer mouse hemoglobins: is there genetic adaptation to high altitude? *BioScience*, **31**, 299–304.

Snyder LRG, Born S, Lechner AJ (1982) Blood oxygen affinity in high- and low-altitude populations of the deer mouse. *Respiration Physiology*, **48**, 89–105.

Stager M, Swanson DL, Cheviron ZA (2015) Regulatory mechanisms of metabolic flexibility in the dark-eyed junco (*Junco hyemalis*). *The Journal of Experimental Biology*, **218**, 767–777.

Steppan SJ, Adkins RM, Anderson J (2004) Phylogeny and divergence-date estimates of rapid radiations in muroid rodents based on multiple nuclear genes. *Systematic Biology*, **53**, 533–553.

Storz JF (2007) Hemoglobin function and physiological adaptation to hypoxia in high-altitude mammals. *Journal of Mammalogy*, **88**, 24–31.

Storz JF, Wheat CW (2010) Integrating evolutionary and functional approaches to infer adaptation at specific loci. *Evolution*, **64**, 2489–2509.

Storz JF, Sabatino SJ, Hoffmann FG *et al.* (2007) The molecular basis of high-altitude adaptation in deer mice. *PLoS Genetics*, **3**, e45.

Storz JF, Runck AM, Sabatino SJ *et al.* (2009) Evolutionary and functional insights into the mechanism underlying high-altitude adaptation of deer mouse hemoglobin. *Proceedings of the National Academy of Sciences of the United States of America*, **106**, 14450–14455.

Storz JF, Runck AM, Moriyama H, Weber RE, Fago A (2010a) Genetic differences in hemoglobin function between highland and lowland deer mice. *The Journal of Experimental Biology*, **213**, 2565–2574.

Storz JF, Scott GR, Cheviron ZA (2010b) Phenotypic plasticity and genetic adaptation to high-altitude hypoxia in vertebrates. *The Journal of Experimental Biology*, **213**, 4125–4136.

Van Sant MJ, Hammond KA (2008) Contribution of shivering and nonshivering thermogenesis to thermogenic capacity for the deer mouse (*Peromyscus maniculatus*). *Physiological and Biochemical Zoology*, **81**, 605–611.

Voineagu I, Wang X, Johnston P *et al.* (2011) Transcriptomic analysis of autistic brain reveals convergent molecular pathology. *Nature*, **474**, 380–384.

Wang Z, Gerstein M, Snyder M (2009) RNA-Seq: a revolutionary tool for transcriptomics. *Nature Reviews Genetics*, **10**, 57–63.

Ward MP, Milledge JS, West JB (1989) *High Altitude Medicine and Physiology*. Chapman and Hall Medical, London.

Whitehead A (2012) Comparative genomics in ecological physiology: toward a more nuanced understanding of acclimation and adaptation. *The Journal of Experimental Biology*, **215**, 884–891.

Whitehead A, Roach JL, Zhang S, Galvez F (2011) Genomic mechanisms of evolved physiological plasticity in killifish distributed along an environmental salinity gradient. *Proceedings of the National Academy of Sciences of the United States of America*, **108**, 6193–6198.

Xu K, Sacharidou A, Fu S *et al.* (2011) Blood vessel tubulogenesis requires Rasip1 regulation of GTPase signaling. *Developmental Cell*, **20**, 526–539.

Zhang B, Horvath S (2005) A general framework for weighted gene co-expression network analysis. *Statistical Applications in Genetics and Molecular Biology*, **4**, 2194–6302.

Z.A.C. designed the research. Z.A.C. and C.J.W. collected field data, and J.J. collected laboratory data and sequenced transcriptomes. J.P.V and Z.A.C. conducted the analysis, interpreted the results and wrote the manuscript.

Data accessibility

Raw sequence reads have been deposited to NCBI's Sequence Read Archive, Accession no. SRP073101. Novel *Peromyscus maniculatus* annotations and NST phenotype data are available in online supporting material.

Supporting information

Additional supporting information may be found in the online version of this article.

Table S1. Weighted Gene Co-expression Network Analysis (WGNCA) module assignments for all genes in the *Peromyscus maniculatus* brown adipose tissue transcriptome (16 406 genes).

Table S2. Results of correlation analysis testing for associations between module expression and non-shivering thermogenesis.

Table S3. Functional enrichment analysis results for all WGCNA modules significantly associated with non-shivering thermogenic performance (see Fig. 5).

Table S4. Results of differential expression analysis on the hub genes of modules associated with non-shivering thermogenesis (see Fig. 6).

Table S5. Results of differential expression analysis of all a priori defined candidate genes.

Table S6. Results of differential expression analysis for vascular endothelial growth factor (VEGF) pathway genes.

Table S7. Table of the percentage of genes significantly ($q < 0.05$) differentially expressed between highland and lowland deer mouse populations within in situ and F_1 conditions for all WGCNA modules significantly associated with non-shivering thermogenic performance (see Fig. 5).

Table S8. Additional *P. maniculatus* gene annotations.

Table S9. Raw and body mass-corrected resting metabolic rate (RMR) and non-shivering thermogenesis (NST) data.

Fig. S1. Analysis of network topology conducted to choose a soft-thresholding power (β).

Fig. S2. Gene co-expression network cluster dendrogram and module detection.

Fig. S3. Venn diagram displaying the number of genes differentially expressed ($q < 0.05$) between highland and lowland deer mice within *in situ* and F_1 conditions.